Research Square

Preprints are preliminary reports that have not undergone peer review.
They should not be considered conclusive, used to inform clinical practice,
or referenced by the media as validated information.

Estimated potential soil CO_2 and N_2O emission dynamics along a narrow elevational gradient in a warm- temperate coastal forest

Li Li

lili028@njfu.edu.cn

Nanjing Forestry University

Qiang Ma

Nanjing Forestry University

Zimiao Zhuang

Nanjing Forestry University

Jiahui Tan

Nanjing Forestry University

Yuanyuan Zhang

Nanjing Institute of Environmental Sciences

Jun Gao

Nanjing Institute of Environmental Sciences

Research Article

Keywords: Elevation gradient, Soil greenhouse-gas emissions, Environmental controls, Warm-temperate forest, Empirical model

Posted Date: November 25th, 2026

DOI: https://doi.org/10.21203/rs.3.rs-11283194/v1

License: This work is licensed under a Creative Commons Attribution 4.0 International License.
Read Full License

Additional Declarations: No competing interests reported.

Estimated potential soil CO_2 and N_2O emission dynamics along a narrow elevational gradient in a warm-temperate coastal forest

Li Li[1,2*], Qiang Ma[1], Zimiao Zhuang[1], Jiahui Tan[1], Yuanyuan Zhang[2], Jun Gao[2*]

[1]State Key Laboratory for Development and Utilization of Forest Food Resources, Bamboo Research institute, Forestry and Grassland School, Nanjing Forestry University, Nanjing, China

[2]Kunyu Mountain Station, Ecological Quality Comprehensive Monitoring Centre, Nanjing Institute of Environmental Science, Ministry of Ecology and Environment, Nanjing 210042, China

[*]Corresponding author: Li Li (lili028@njfu.edu.cn) and Jun Gao (gaojun@nies.org).

Abstract: Soil greenhouse gas emissions may vary across short elevational gradients, but their controls remain unclear in humid coastal forests. We investigated soils from three elevations in a warm-temperate forest of Kunyu Mountain, China (217, 302 and 411 m). Laboratory incubations were used to derive Q_{10} values for CO_2 and N_2O emissions, which were combined with field meteorological data and moisture correction functions to estimate monthly, seasonal and annual emissions. Redundancy analysis was then used to identify soil factors associated with emission variation. Annual mean potential CO_2 emission rates declined significantly with elevation, with rates at the low-elevation site 83.8% and 241.0% higher than those at the middle- and high-elevation sites, respectively. CO_2 emissions were higher in the growing season than in the non-growing season at all elevations, and the seasonal increase was strongest at the high-elevation site. In contrast, annual mean N_2O emission rates did not differ significantly among elevations, although high-elevation soils emitted more N_2O than middle-elevation soils during the middle and late growing season. Carbon-normalized CO_2-C emission intensity decreased with elevation, whereas nitrogen-normalized N_2O-N loss intensity was highest at high elevation, about four times that at middle elevation. Redundancy analysis identified soil pH as the strongest independent explanatory factor for CO_2 emissions (65.9%, $P = 0.01$) and soil total nitrogen stock as the main factor for N_2O emissions (50.2%, $P = 0.02$). These findings suggest that soil properties, substrate availability, stand characteristics and microclimate, rather than temperature alone, shape soil greenhouse gas emissions along narrow elevational gradients.

Keywords: Elevation gradient; Soil greenhouse-gas emissions; Environmental controls; Warm-temperate forest; Empirical model

1. Introduction

Forest soils are a key component of terrestrial carbon and nitrogen cycling. Their CO_2 and N_2O emissions represent gaseous losses associated with soil organic carbon mineralization and nitrogen transformation processes, respectively, and have important impacts on the global greenhouse gas budget (Bonan 2008; Tian et al. 2020). Under ongoing climate warming, accurately estimating the temporal dynamics and spatial patterns of forest soil greenhouse gas emissions is an important prerequisite for predicting terrestrial ecosystem feedbacks to climate change (IPCC 2023). However, CO_2 and N_2O are produced through distinct mechanisms. CO_2 mainly originates from soil organic matter decomposition and root and microbial respiration and is jointly regulated by temperature, carbon substrate availability, and microbial activity (Davidson and Janssens 2006). In contrast, although N_2O production is also influenced by carbon availability, it mainly occurs through nitrification and denitrification and is jointly controlled by nitrogen substrate supply, soil moisture, oxygen diffusion, and local anaerobic microsites (Butterbach-Bahl et al. 2013; Lacroix et al. 2023). Because their production processes and environmental controls differ, CO_2 and N_2O may show contrasting responses to the same environmental gradient. Therefore, simultaneously analyzing the spatial patterns and environmental controls of CO_2 and N_2O emissions within the same ecosystem can improve our understanding of how soil carbon mineralization and nitrogen transformation respond to environmental change.

Elevational gradients provide a natural experimental system for investigating environmental controls on forest soil greenhouse gas emissions because they involve systematic changes in temperature, moisture, vegetation composition, and soil development conditions (Körner 2007). In general, increasing elevation is accompanied by decreasing air temperature, which can reduce microbial metabolic activity and organic matter decomposition rates and thereby suppress

soil CO_2 emissions (Schindlbacher et al. 2010). Meanwhile, the temperature sensitivity of soil organic carbon decomposition may increase under low-temperature conditions, leading to stronger seasonal responses of high-elevation soils during the growing season (Okello et al. 2023). However, in low-mountain forest ecosystems with narrow elevational ranges and maritime climatic influence, the temperature gradient may be relatively weak, making it unclear whether temperature alone can explain spatial variation in soil CO_2 emissions. Soil pH is another important regulator of microbial activity and community composition, and variation in pH can alter the abundance and activity of bacterial and fungal decomposers and consequently influence soil organic matter decomposition and CO_2 production. By contrast, the elevational response of N_2O is usually more complex because its production and consumption processes depend not only on temperature but also strongly on nitrogen availability, moisture status, soil structure, and the formation of anaerobic microsites (Ball 2013; Butterbach-Bahl et al. 2013; Liao et al. 2024).

Long-term continuous in situ measurements of greenhouse gas fluxes can directly reflect ecosystem emission processes, but in mountain forests they are often constrained by complex terrain, difficulties in synchronizing observations among plots, and high monitoring costs (Luo and Zhou 2006). Empirical models based on reference-temperature emission rates and Q_{10} parameters obtained from laboratory incubation, combined with field meteorological data, provide a feasible approach for estimating seasonal and annual dynamics of soil greenhouse gas emissions (Lloyd and Taylor 1994; Meyer et al. 2018). These models integrate incubation-derived temperature sensitivity parameters with field meteorological variation, enabling estimation of emissions across different time scales when continuous in situ flux measurements are unavailable (Chen et al. 2009; Zhang et al. 2015). For N_2O, empirical models also need to account for the regulation of nitrification, denitrification, and gas diffusion by moisture conditions (Butterbach-Bahl et al. 2013). Therefore, combining temperature sensitivity parameters with meteorological moisture correction can provide a quantitative approach for estimating the temporal dynamics and elevational patterns of forest soil CO_2 and N_2O emissions. Further

combining this approach with soil physicochemical analysis can help identify the environmental factors associated with their spatial variation.

Mount Kunyu is located at the eastern end of the Shandong Peninsula and is characterized by a maritime warm-temperate humid climate and acidic brown soils developed from granite parent material. It is also an important natural distribution area of *Pinus densiflora* in China (Fang et al. 2018). Compared with high-elevation mountains or inland forests, Mount Kunyu is a relatively low-elevation mountain system, with a limited elevational range. The three study elevations (217–411 m) therefore represent a relatively narrow but environmentally meaningful elevational gradient within this maritime forest system. Despite the relatively small elevational difference, soil physicochemical properties, stand characteristics, and the relative abundance of associated plant species may vary among elevations, potentially contributing to spatial variation in soil CO_2 and N_2O emissions. Thus, the *Pinus densiflora* forests of Mount Kunyu provide a useful setting for examining whether soil greenhouse gas emissions exhibit appreciable spatial differentiation across a relatively narrow elevational gradient under maritime climatic influence. In addition, the region is strongly influenced by the East Asian monsoon, with pronounced seasonal differences in temperature and atmospheric moisture, providing suitable conditions for estimating seasonal dynamics of soil greenhouse gas emissions using empirical models. However, systematic studies of the elevational patterns and environmental controls of soil CO_2 and N_2O emissions in this maritime warm-temperate forest ecosystem remain limited.

Based on this background, this study investigated warm-temperate forest soils at three elevations in Mount Kunyu (217, 302, and 411 m). CO_2 and N_2O emission rates and Q_{10} parameters obtained from laboratory incubation under varying temperatures were combined with field temperature and atmospheric humidity data to construct an empirical model for estimating monthly, seasonal, and annual soil CO_2 and N_2O emissions. Redundancy analysis (RDA) was then used to identify key soil environmental factors based on soil total carbon (TC), total nitrogen (TN), pH, and C/N ratio. This study

addressed three main questions: (1) whether soil CO_2 emissions in a maritime warm-temperate forest with a narrow elevational range still show the classical decreasing pattern with increasing elevation; (2) whether spatial variation in CO_2 emissions is primarily associated with temperature variation or with differences in soil physicochemical properties; and (3) whether N_2O emissions show an elevational response different from that of CO_2 because of their dependence on nitrogen status and moisture conditions. We hypothesized that soil CO_2 emissions would decrease with increasing elevation, but that their spatial variation would be more strongly associated with soil environmental conditions than with the relatively weak temperature gradient. In contrast, because N_2O production depends strongly on nitrogen availability and moisture conditions, N_2O emissions were expected to show a different elevational response from CO_2, reflecting contrasting environmental controls on soil carbon mineralization and nitrogen transformation processes.

2. Materials and methods

2.1 Study site and soil sampling

The study was conducted in the Kunyu Mountain National Nature Reserve, Yantai, Shandong Province, China (37°11′–37°17′ N, 121°40′–121°48′ E). The reserve is an important natural distribution area of *Pinus densiflora* in China and serves as an ecological barrier on the Shandong Peninsula. Kunyu Mountain lies within the warm-temperate coastal transition zone and is characterized predominantly by acidic brown forest soils, with a maximum elevation of 923 m above sea level. Based on the topography and elevational distribution of the study area, three elevation sites were selected at 217 m (LE), 302 m (ME), and 411 m (HE) above sea level. The forest stands at all three elevations were dominated by *Pinus densiflora*, although the relative abundance of associated plant species varied among sites.

At each elevation, three spatially separated 50 m × 50 m plots were established on sunny slopes with similar slope positions and relatively homogeneous vegetation cover. The minimum distance between plots was 50 m, and all plots were subject to minimal human disturbance. Within each plot, three 1 m × 1 m subplots, spaced approximately 3 m apart,

were established to account for within-plot spatial heterogeneity. Soil samples were collected from the 0–10 cm layer in April 2024. Within each subplot, soil was collected from three randomly selected positions. Samples collected from the nine positions within each plot were thoroughly homogenized to form one composite sample. Thus, three independent plot-level composite samples were obtained at each elevation.

A preliminary incubation experiment indicated that CO_2 and N_2O production was substantially lower in the 10–20 and 20–30 cm soil layers than in the 0–10 cm layer. Therefore, the subsequent analyses focused on the upper 0–10 cm soil layer, where soil biological activity and gas production were expected to be comparatively high.

2.2 Measurements

2.2.1 Temperature sensitivity (Q_{10}) of soil CO_2 and N_2O emissions

The temperature sensitivity (Q_{10}) of soil CO_2 and N_2O emissions was determined using laboratory incubation under controlled temperature conditions (Online Resource 1; Figs. S1–S2). A preliminary experiment indicated that incubation temperatures above 28 °C substantially altered soil properties; therefore, five incubation temperatures (0, 7, 14, 21, and 28 °C) were selected to encompass the temperature range likely to occur in the study area. Each temperature treatment had three replicates and was incubated for 72 h. Greenhouse gas fluxes were measured periodically to calculate the Q_{10} values of soils from different elevations.

After sampling, soils were stored at 4 °C for 10 days. Three soil samples were collected from each site, air-dried, and 100 g of soil (0–10 cm) was placed into a 500 mL screw-cap glass bottle. Soil moisture was adjusted to 50% of field water-holding capacity, and the soils were pre-incubated at 20 °C for 3 days to stabilize microbial activity prior to the temperature treatments. The incubation temperatures were applied in a randomized sequence (7, 28, 14, 0, and 21 °C). Independent soil samples were used for each temperature treatment to avoid substrate depletion. After each incubation, the soils were retained for subsequent physicochemical analyses. Soil water content was maintained at 50% of field

water-holding capacity by regularly weighing the samples and adding deionized water to compensate for water loss. The incubation vessels were not sealed, allowing gas exchange with the surrounding atmosphere and minimizing the potential for O_2 depletion during incubation.

At each of the five temperature levels, three replicate soil samples were incubated for each elevation. Headspace gas samples were collected using a syringe at 0, 5, and 15 min after chamber closure. Gas concentrations were determined using a gas chromatograph (Agilent 7890B, USA), and CO_2 and N_2O fluxes were calculated from the linear changes in gas concentrations over the incubation period. The resulting fluxes were used to determine the temperature sensitivities (Q_{10}) of CO_2 and N_2O emissions (Online Resource 1; Figs. S1–S2).

The relationship between CO_2 mineralization rate and incubation temperature was described using a first-order exponential model:

$$F=a\times e^{bt} \tag{1}$$

where F is the CO_2 mineralization rate, a is the mineralization rate at 0 °C, t is the incubation temperature (°C), and b is the temperature response coefficient.

The temperature sensitivity (Q_{10}) was calculated as:

$$Q_{10}=e^{10b} \tag{2}$$

where b is the temperature response coefficient. The same equation was used to calculate the Q_{10} value for N_2O emissions. Although N_2O emissions are strongly regulated by soil moisture, the temperature response component was quantified using the same exponential function to parameterize temperature sensitivity under controlled moisture conditions.

The CO_2 mineralization rate was calculated as:

$$F=d_c/d_t\times V_H/W_S\times M_W/M_V\times T_{ST}/(T_{ST}+T_1) \tag{3}$$

where F is the CO_2 mineralization rate (mg kg^{-1} h^{-1}); d_c/d_t is the rate of change in gas concentration (ppm h^{-1}), obtained from linear regression of gas concentrations measured at the three sampling times after chamber closure; V_H is the headspace volume (L), calculated as the effective bottle volume after subtracting the volume occupied by soil and added water; W_S is the dry soil mass (g); M_W is the molecular weight of CO_2 (44 g mol^{-1}); M_V is the molar volume of an ideal gas under standard conditions (22.4 L mol^{-1}); T_{ST} is the absolute temperature (273.15 K); and T_1 is the incubation temperature (°C). The N_2O emission rate was calculated using the same equation.

2.2.2 Estimation of field soil CO_2 and N_2O emission rates

Field soil CO_2 and N_2O emission rates were estimated using an empirical model based on the emission rate at a reference temperature and the Q_{10} temperature-sensitivity coefficient (Meyer et al. 2018):

$$R=R_{ref}\times Q_{10}^{(T-T_{ref})/10}\times SD\times H\times f_{(W_{soil})} \quad (4)$$

where R is the estimated soil CO_2 or N_2O emission rate (mg m^{-2} h^{-1}); R_{ref} is the soil emission rate measured during laboratory incubation at the reference temperature (T_{ref} = 10 °C) (mg kg^{-1} h^{-1}); T is the daily soil temperature (°C) at each elevation; SD is soil bulk density (kg m^{-3}); H is the soil depth (0.1 m); and $f(W_{soil})$ is the soil moisture correction function. R_{ref} is the interpolated soil emission rate at the reference temperature (T_{ref} = 10 °C), derived from the fitted exponential temperature-response model using the five incubation temperatures of 0, 7, 14, 21, and 28 °C, rather than a directly measured value. Daily soil temperature and soil water content data for 2024 were obtained from the local meteorological station.

For CO_2 emissions, relative soil water content was used as the moisture correction factor:

$$f_{(W_{soil})}=W_{soil}/W_{ref} \quad (5)$$

where W_{soil} is the soil water content at each elevation and W_{ref} is the reference soil water content used during laboratory incubation. This approach follows previous soil respiration models in which relative soil moisture is used to characterize water availability. Continuous soil water contents of three elevation sites were monitored in 2024.

2.2.3 Soil pH and bulk density

Soil pH was determined potentiometrically. Briefly, 10 g of air-dried soil passed through a 2-mm sieve was placed in a beaker, and deionized water was added at a soil to water ratio of 1:2.5 (w/v). The suspension was shaken for 30 min and then allowed to stand until it reached a relatively stable state. Soil pH was measured using a pH meter after calibration with standard buffer solutions. Each sample was measured in duplicate, and the mean value was used for subsequent analyses (Rolka and Wyszkowski 2021). Soil bulk density was determined using the core method and calculated from the oven-dry soil mass and core volume.

2.2.4 Soil carbon and nitrogen stocks

Soil carbon (C) and nitrogen (N) stocks were calculated from soil C and N concentrations, bulk density, and soil layer thickness. Total soil C and N concentrations were determined using an elemental analyzer (Multi N/C 2100S, Analytik Jena AG, Germany). Finely ground soil samples were weighed to the nearest 0.1 mg and analyzed according to the manufacturer's instructions.

2.2.5 CO_2-C emission intensity per unit soil carbon stock and N_2O-N loss intensity per unit soil nitrogen stock

The CO_2-C emission intensity normalized by total carbon (TC) stock was calculated as:

$$I_{CO_2} = F_{CO_2\text{-}C} / S_{TC} \quad (6)$$

Where I_{CO_2} is the TC-normalized CO_2-C emission intensity (kg C kg^{-1} TC yr^{-1}), $F_{CO_2\text{-}C}$ is the cumulative annual CO_2-C emission (kg C m^{-2} yr^{-1}), and S_{TC} is the TC stock in the 0–10 cm soil layer (kg C m^{-2}).

The N_2O-N loss intensity normalized by total nitrogen (TN) stock was calculated as:

$$I_{N_2O} = F_{N_2O\text{-}N} / S_{TN} \quad (7)$$

Where I_{N_2O} is the TN-normalized N_2O-N loss intensity (kg N kg^{-1} TN yr^{-1}), $F_{N_2O\text{-}N}$ is the cumulative annual N_2O-N emission (kg N m^{-2} yr^{-1}), and S_{TN} is the TN stock in the 0–10 cm soil layer (kg N m^{-2}).

2.3 Data analysis

Raw data were first organized, converted to consistent units, and used to calculate derived variables in Microsoft Excel 2019. Before statistical analysis, all variables were tested for normality and homogeneity of variance. Data meeting the assumptions of parametric tests were subjected to analysis of variance. For variables involving both elevation and season, CO_2 and N_2O emissions during the growing and non-growing seasons were analyzed using two-way analysis of variance (two-way ANOVA). Other variables were analyzed using one-way ANOVA. Duncan's multiple range test was used for post hoc comparisons among elevations, with statistical significance set at $P < 0.05$. Differences between the growing and non-growing seasons were evaluated using paired-samples t-tests.

Redundancy analysis (RDA) was further performed to identify the contributions of environmental factors to soil CO_2 and N_2O emissions across elevations. Analysis of variance and Pearson correlation analysis were conducted using SPSS Statistics 27.0 (IBM Corp., Armonk, NY, USA). RDA and ordination diagrams were performed using CANOCO 5.0 (Microcomputer Power, Ithaca, NY, USA). Bar charts and line graphs were generated using SigmaPlot 2024 (Systat Software Inc., San Jose, CA, USA).

3. Results

3.1 Estimated Monthly Emissions

The empirical model estimates showed that soil CO_2 emission rates exhibited clear monthly dynamics and elevational differences (Fig. 1a). CO_2 emissions increased during the growing season at all three elevations, reached relatively high levels in July–August, and then gradually declined. Except in a few months, CO_2 emission rates at LE were significantly

higher than those at ME and HE, with an overall pattern of LE > ME > HE, indicating a decreasing trend in CO_2 emissions with increasing elevation. Differences between ME and HE mainly occurred from January to April and in December, whereas differences between the two elevations were weak or not significant in the remaining months.

N_2O emissions showed a monthly dynamic pattern different from that of CO_2 (Fig. 1b). N_2O emissions mainly increased during the middle and late growing season and reached relatively high levels from July to September. From June to September, N_2O emission rates at HE were significantly higher than those at ME, whereas no significant differences were observed between HE and LE. In the other months, differences among the three elevations were weak. These results indicate that the elevational response of N_2O emissions did not show the same decreasing trend as CO_2 emissions.

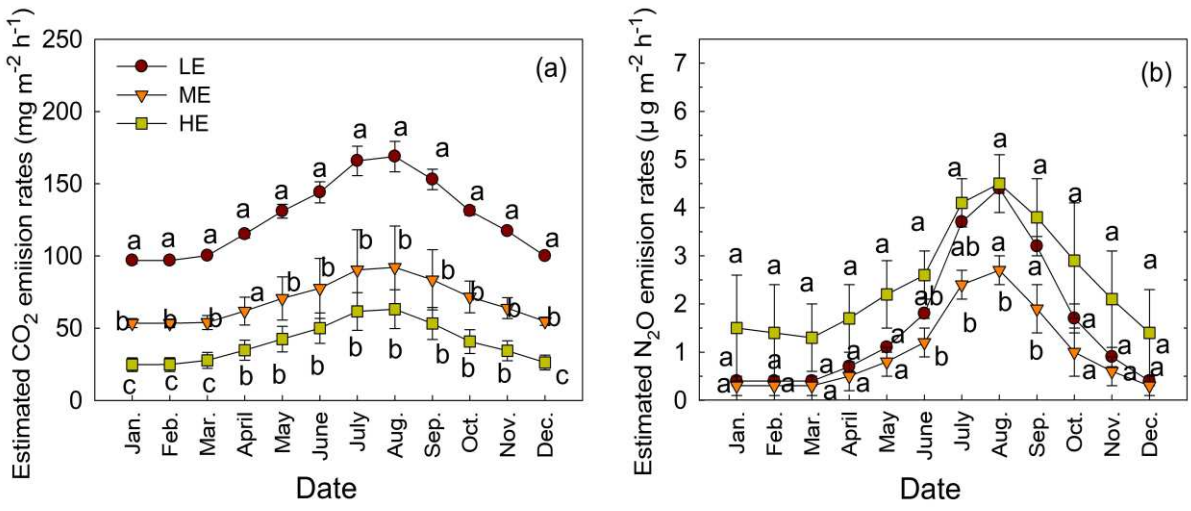

Fig. 1 Monthly dynamics of estimated CO_2 and N_2O emission rates across elevations

Values are means ± SD. Asterisks indicate significant elevation effects based on one-way ANOVA at $P < 0.05$. Different lowercase letters indicate significant differences among elevations within the same month at $P < 0.05$

3.2 Estimated CO_2 and N_2O Emissions During the Growing Season and Non-Growing Season

Two-way ANOVA showed that both season and elevation had highly significant effects on CO_2 emission rates, whereas their interaction was not significant (Fig. 2a). CO_2 emission rates decreased significantly with increasing elevation, following the order LE > ME > HE. At all three elevations, CO_2 emission rates were significantly higher during the

growing season than during the non-growing season, indicating clear seasonal variation in CO_2 emissions. CO_2 emissions at HE showed a stronger seasonal response, with growing-season increases relative to the non-growing season of 36.60%, 35.73%, and 70.81% at LE, ME, and HE, respectively.

N_2O emission rates were also significantly affected by season and elevation, while the interaction between season and elevation was not significant (Fig. 2b). In contrast to CO_2, N_2O emission rates were highest at HE and were significantly higher than those at LE and ME, whereas no significant difference was observed between LE and ME. N_2O emissions also showed clear seasonal variation, with significantly higher emission rates during the growing season than during the non-growing season at all elevations. The growing-season increases in N_2O emissions were 257.14%, 220.00%, and 77.78% at LE, ME, and HE, respectively.

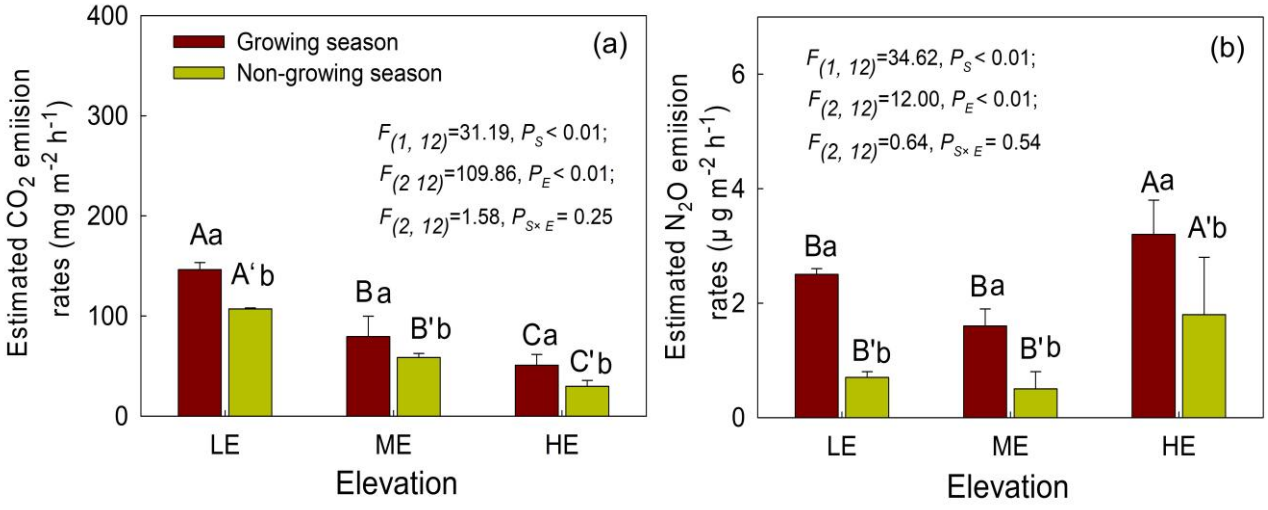

Fig. 2 Estimated CO_2 and N_2O emission rates during the growing and non-growing seasons across elevations

Values are means ± SD. Different uppercase letters indicate significant differences among elevations within the same season, whereas different lowercase letters indicate significant differences between the growing and non-growing seasons within the same elevation ($P < 0.05$). S, E, and S × E indicate the effects of season, elevation, and their interaction, respectively

3.3 Soil Total Carbon Stock, Total Nitrogen Stock, C/N Ratio, and pH

Soil total carbon (TC) stock in the 0–10 cm layer did not differ significantly among elevations (Fig. 3a). Soil total nitrogen (TN) stock was significantly lower at HE than at LE and ME; compared with ME and LE, TN stock at HE decreased by 30.89% and 32.45%, respectively (Fig. 3b). Soil C/N ratio increased with elevation, with HE being significantly higher than LE by 64.65%; ME showed an intermediate value and did not differ significantly from either LE or HE (Fig. 3c). In addition, soil pH was highest at LE and was significantly higher than those at ME and HE, whereas no significant difference was observed between ME and HE (Fig. 3d).

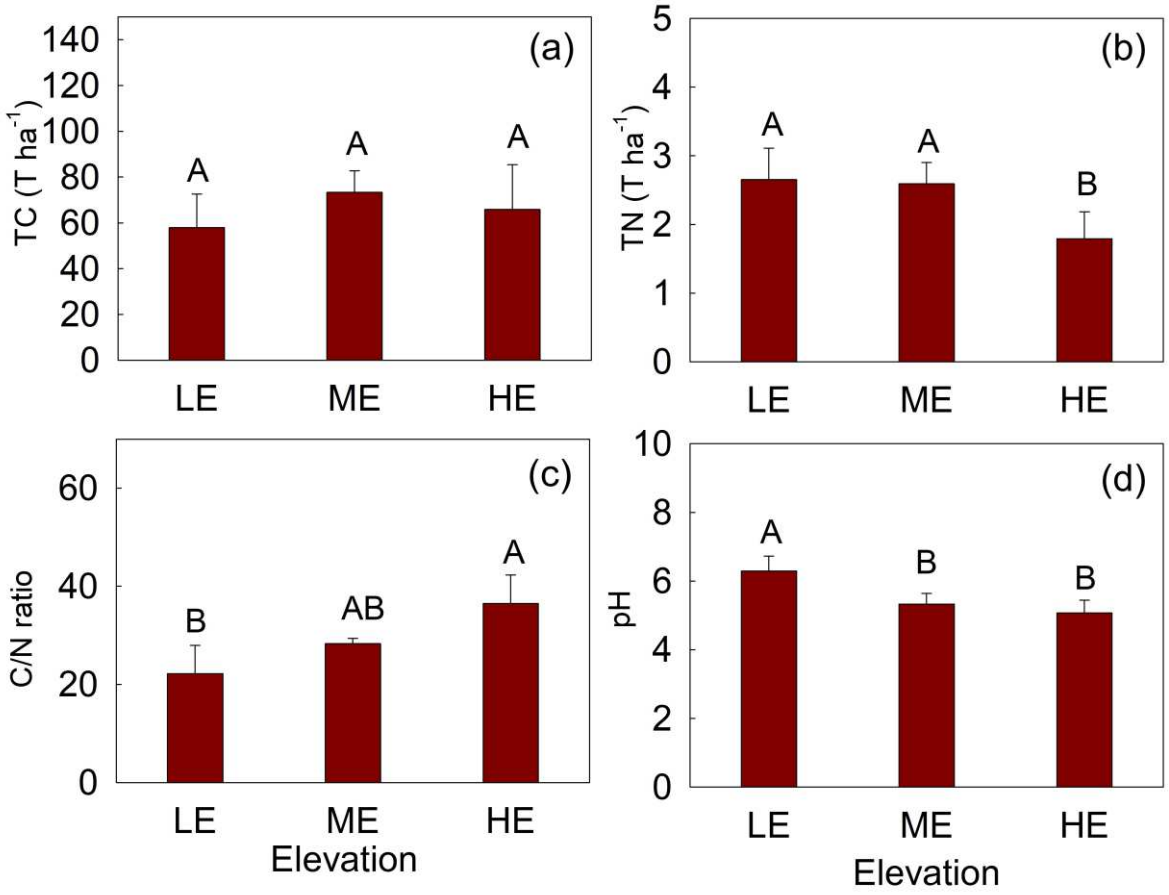

Fig. 3 Soil total carbon stock, total nitrogen stock, C/N ratio and pH value across elevations

Values are means ± SD. Different uppercase letters indicate significant differences among elevations at $P < 0.05$

3.4 TC-Normalized CO_2-C Emission Intensity and TN-Normalized N_2O-N Loss Intensity

The results showed significant differences in TC-normalized CO_2-C emission intensity among elevations. TC-normalized CO_2-C emission intensity gradually decreased with increasing elevation, following the order LE > ME > HE. Compared

with LE and ME, the value at HE decreased by 72.00% and 57.14%, respectively (Fig. 4a). TN-normalized N_2O-N loss intensity was highest at HE and was significantly higher than that at ME, approximately four times the value at ME. LE showed an intermediate value and did not differ significantly from either HE or ME (Fig. 4b).

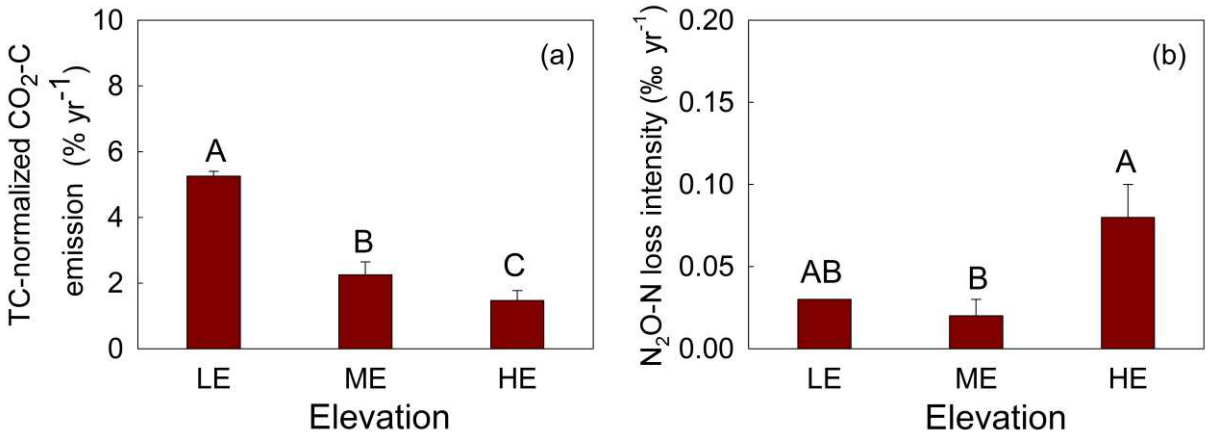

Fig. 4 TC-normalized CO_2-C emission (a) and TN-normalized N_2O-N loss intensity (b) across elevations

Values are means ± SD. Different uppercase letters indicate significant differences among elevations at $P < 0.05$

3.5 Effects of environmental factors

RDA results showed that RDA1 and RDA2 explained 77.07% and 0.47% of the total variation, respectively. Estimated CO_2 emissions during different seasons and across the whole year showed consistent directions in the ordination space and were closely aligned with pH, indicating that pH was the main soil factor associated with the spatial variation in CO_2 emissions (Fig. 5). Forward selection further showed that pH independently explained 65.9% of the variation in CO_2 emissions, contributing 83.8% of the explained variation, and reached statistical significance (Pseudo-F = 13.0, $P = 0.01$, Table 1). In contrast, TC, TN, and C/N explained relatively small proportions of the variation and were not statistically significant (Fig. 5, Table 1).

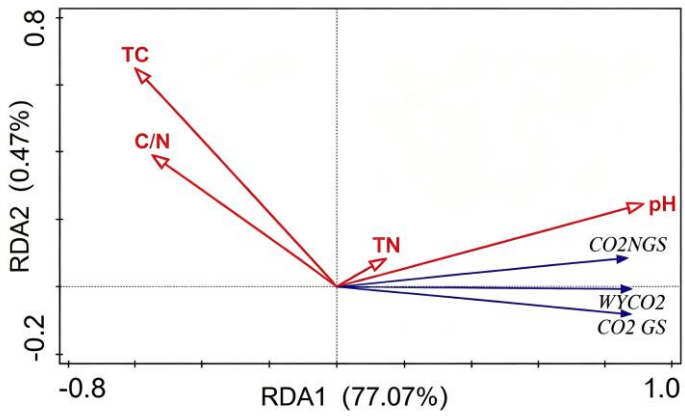

Fig. 5 Redundancy analysis (RDA) of estimated CO_2 emissions and soil environmental factors

GS, growing season; NGS, non-growing season; WY, whole year

Table 1 Explanatory contribution of environmental factors to CO_2 emissions

Variable	Explains (%)	Contribution (%)	Pseudo-F	P-value
pH	65.9	83.8	13.0	0.01
TC	3.7	4.8	0.7	0.41
TN	8.5	11.0	1.5	0.30
C/N	0.3	0.4	＜0.1	0.82

RDA results showed that the first two axes explained 64.41% and 1.47% of the total variation, respectively (Fig.6, Table 2). Forward selection indicated that soil TN was the dominant explanatory factor, accounting for 50.2% of the variation and 76.2% of the explained contribution (Pseudo-F = 7.1, P = 0.024). In contrast, soil TC, pH, and soil C/N explained relatively small proportions of the variation and were not significant ($P > 0.05$).

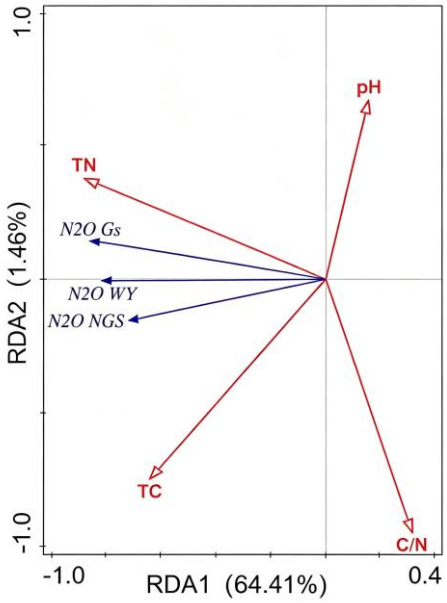

Fig. 6 Redundancy analysis (RDA) of estimated N_2O emissions and soil environmental factors

Table 2 Explanatory contribution of environmental factors to N_2O emissions

Variable	Explains (%)	Contribution (%)	Pseudo-F	P-value
TN	50.2	76.2	7.1	0.02
TC	10.5	16.0	1.6	0.23
pH	2.6	3.9	0.3	0.61
C/N	2.6	3.9	0.3	0.65

4. Discussion

4.1 Elevational pattern of CO_2 emissions and its relationship with soil pH

The estimated results showed that both annual mean potential soil CO_2 emission rates and cumulative annual CO_2 emissions decreased from LE to HE, following the order LE > ME > HE. The annual mean emission rate at LE was

83.76% and 241.00% higher than those at ME and HE, respectively. This pronounced difference occurred across a relatively narrow elevational gradient of only 194 m, indicating substantial spatial variation in potential soil CO_2 emissions within the studied low-elevation *Pinus densiflora* forest. Although all three elevations were dominated by *Pinus densiflora*, differences in soil physicochemical properties, stand characteristics, the relative abundance of associated plant species, and local microclimatic conditions may also have contributed to the observed variation. In addition, the humid maritime climate of Mount Kunyu may reduce temperature differences across this narrow elevational range. Therefore, the observed CO_2 pattern should be interpreted as an association with elevation rather than as evidence of a direct temperature-driven effect of elevation alone.

The RDA results showed that, among the measured soil physicochemical variables, pH had the highest explanatory power for the spatial variation in CO_2 emissions, accounting for 65.9%, whereas the independent explanatory effects of TC, TN, and C/N were not significant. This indicates a strong association between soil pH and CO_2 emissions. The possible explanation was that soil pH may affect organic carbon stabilization and accessibility through interactions between organic matter and mineral surfaces (Lützow et al. 2006; Lehmann et al. 2020).

The TC-normalized CO_2-C emission intensity also decreased significantly with increasing elevation. Because soil TC stocks did not differ significantly among elevations, total carbon pool size alone was insufficient to explain the observed emission pattern. Other unmeasured characteristics of soil carbon quality and substrate availability may have contributed to the spatial variation in CO_2 emissions. Yi et al. (2018) found that soil CO_2 emissions in a *Pinus tabuliformis* forest in the Qinling Mountains were associated with soil temperature, moisture, and texture.

4.2 Contrasting elevational response of N_2O and its relationship with soil nitrogen status

Unlike CO_2 emissions, annual mean N_2O emission rates did not show a monotonic elevational pattern. However, N_2O emissions at HE were relatively high during the middle and late growing season, and TN-normalized N_2O-N emission intensity was highest at HE, approximately four times that at ME.

The RDA results showed that TN had the highest independent explanatory power for the spatial variation in N_2O emissions. However, bulk TN represents the overall soil nitrogen pool rather than the immediate substrates of nitrification and denitrification, such as NH^{4+} and NO^{3-}, which were not measured. Therefore, the association between TN and N_2O emissions may reflect broader differences in soil nitrogen status and other site-associated conditions rather than a direct effect of TN. Seasonal measurements of inorganic nitrogen and soil moisture would be needed to identify the proximal controls of N_2O production.

Interestingly, TN-normalized N_2O-N emission intensity was highest at HE despite its lower TN stock. This indicates relatively high estimated N_2O-N loss in relation to the size of the soil TN pool at HE. The pattern may reflect differences in nitrogen availability, hydrothermal conditions, or other unmeasured soil properties. Yi et al. (2018) reported N_2O fluxes of 5.59-9.57 μg m^{-2} h^{-1} across slope positions in a *Pinus tabuliformis* forest in the Qinling Mountains and found that nitrate availability, and soil texture were associated with N_2O emissions.

4.3 Seasonal differences in CO_2 and N_2O responses

Both CO_2 and N_2O emissions showed clear seasonal variation, with higher estimated emission rates during the growing season than during the non-growing season. The relative increase in CO_2 emissions was greatest at HE, reaching 70.81%, compared with 36.61% at LE and 35.71% at ME. Thus, although annual CO_2 emissions were lower at HE, the estimated seasonal increase was proportionally greater.

The proportionally greater seasonal increase in estimated CO_2 emissions at HE is broadly consistent with the temperature sensitivity of soil organic matter decomposition (Davidson and Janssens 2006; Okello et al. 2023). However, because seasonal dynamics were estimated using an empirical model rather than continuous field flux measurements, this pattern should be interpreted as a difference in estimated seasonal response rather than direct evidence of stronger microbial responses or field temperature sensitivity at HE.

In contrast, growing-season increases in N_2O emissions at LE and ME reached 257.1% and 220.0%, respectively, compared with 77.8% at HE. Seasonal N_2O dynamics are influenced by temperature together with nitrogen availability, moisture conditions, oxygen diffusion, and anaerobic microsites (Butterbach-Bahl et al. 2013; Liao et al. 2024). The stronger estimated seasonal increase at LE and ME may therefore reflect differences in the combination of environmental conditions among elevations. However, because mineral nitrogen was not measured, the specific factors responsible cannot be resolved.

Unlike the winter N_2O emission peaks reported by Yi et al. (2018) for a *Pinus tabuliformis* forest in the Qinling Mountains, the present estimates indicated higher N_2O emissions mainly during the growing season. However, direct comparison should be made cautiously because the two studies used different measurement and estimation approaches.

Because seasonal variation in the present study was estimated using an empirical model incorporating Q_{10} parameters and temperature and humidity, the results primarily provide estimates of temporal patterns rather than direct observations of field flux dynamics. The approach nevertheless provides a useful framework for exploring seasonal variation when continuous in situ measurements are unavailable.

4.4 Methodological limitations

Several limitations should be considered. First, the modeled CO_2 emissions mainly represent potential microbial CO_2 production under standardized incubation conditions rather than total field soil respiration, which also includes root respiration. Second, although all plots were located in *Pinus densiflora*-dominated forests, elevation effects could not be completely separated from unmeasured differences in stand characteristics and local environmental conditions. Therefore, the relationships between soil properties and estimated emissions should be interpreted as associations rather than evidence of direct causal controls. Finally, air-drying and rewetting the soils to 50% WHC may have induced a Birch-effect pulse, potentially affecting the estimated R_{ref} and Q_{10} values. The incubation-derived parameters should therefore be regarded as standardized laboratory estimates rather than direct field-flux parameters.

5. Conclusions

This study combined laboratory-derived emission rates and temperature-sensitivity parameters with field meteorological data to estimate potential soil CO_2 and N_2O emissions along a narrow elevational gradient in the maritime warm-temperate *Pinus densiflora* forests of Mount Kunyu. Soil CO_2 emissions declined significantly with increasing elevation, whereas N_2O emissions showed no corresponding decreasing trend. Soil pH was the strongest explanatory variable for CO_2 emissions, while total nitrogen (TN) showed the highest explanatory power for N_2O emissions, suggesting different site-level associations for the two gases. Potential CO_2 and N_2O emissions differed among the three elevations, despite the narrow elevational range. The empirical model provides a useful framework for incorporating such variation into regional carbon and nitrogen budget assessments. Future studies combining in situ flux observations across multiple maritime mountain sites are needed to validate and generalize these findings.

Statements and Declarations

Acknowledgments: The authors thank the field staff of Kunyu Mountain National Nature Reserve for logistical support during soil sampling, and the Kunyu Mountain Ecological Monitoring Station for providing the field meteorological datasets used in this study.

Author Contributions: LL: Conceptualization, Data curation, Data analysis, Funding acquisition, Methodology, Project administration, Resources, Supervision, Writing – original draft preparation, Writing – review and editing. QM: Investigation, Laboratory analyses, Data curation, Methodology, Writing – original draft preparation. ZZ and JT: Methodology. YZ: Resources, Supervision. JG: Methodology, Writing – review and editing, Resources, Funding acquisition.

Funding: This study was supported by the Open Foundation of Kunyu Mountain Station of Ecological Quality Comprehensive Monitoring Centre, Ministry of Ecology and Environment (No. NIES-KYS-202401), and the Special Fund of Chinese Central Government for Basic Scientific Research Operations in Commonweal Research Institute

(GYZX250103, GYZX250208, GYZX250209).

Data Availability: The datasets generated during and/or analysed during the current study are available from the corresponding author on reasonable request.

Competing interests: The authors have no relevant financial or non-financial interests to disclose.

References

Ball, B. C. 2013. Soil structure and greenhouse gas emissions: A synthesis of 20 years of experimentation. *European Journal of Soil Science* 64(3): 357–373. https://doi.org/10.1111/ejss.12013

Bonan, G. B. 2008. Forests and climate change: Forcings, feedbacks, and the climate benefits of forests. *Science* 320(5882): 1444–1449. https://doi.org/10.1126/science.1155121

Butterbach-Bahl, K., E. M. Baggs, M. Dannenmann, R. Kiese, and S. Zechmeister-Boltenstern. 2013. Nitrous oxide emissions from soils: How well do we understand the processes and their controls? *Philosophical Transactions of the Royal Society B: Biological Sciences* 368(1621): 20130122. https://doi.org/10.1098/rstb.2013.0122

Chen, S., Y. Huang, and J. Zou. 2009. Daily heterotrophic respiration model considering the diurnal temperature variability in the soil. *Journal of Geophysical Research: Biogeosciences* 114: G01022. https://doi.org/10.1029/2008JG000834

Davidson, E. A., and I. A. Janssens. 2006. Temperature sensitivity of soil carbon decomposition and feedbacks to climate change. *Nature* 440(7081): 165–173. https://doi.org/10.1038/nature04514

Fang, J., H. Song, Y. Zhang, Y. Li, and J. Liu. 2018. Climate-dependence of ecosystem services in a nature reserve in northern China. *PLOS ONE* 13(2): e0192727. https://doi.org/10.1371/journal.pone.0192727

IPCC. 2023. Climate change 2023: Synthesis report. Contribution of Working Groups I, II and III to the Sixth Assessment Report of the Intergovernmental Panel on Climate Change. IPCC, Geneva, Switzerland.

https://doi.org/10.59327/IPCC/AR6-9789291691647

Körner, C. 2007. The use of 'altitude' in ecological research. *Trends in Ecology & Evolution* 22(11): 569–574. https://doi.org/10.1016/j.tree.2007.09.006

Lacroix, E. M., M. Aeppli, K. Boye, E. Brodie, S. Fendorf, M. Keiluweit, H. R. Naughton, V. Noël, D. Sihi, and A. Thompson. 2023. Consider the anoxic microsite: Acknowledging and appreciating spatiotemporal redox heterogeneity in soils and sediments. *ACS Earth and Space Chemistry* 7(9): 1592–1609. https://doi.org/10.1021/acsearthspacechem.3c00032

Lehmann, J., C. M. Hansel, C. Kaiser, M. Kleber, K. Maher, S. Manzoni, N. Nunan, M. Reichstein, J. P. Schimel, M. S. Torn, W. R. Wieder, and I. Kögel-Knabner. 2020. Persistence of soil organic carbon caused by functional complexity. *Nature Geoscience* 13(8): 529–534. https://doi.org/10.1038/s41561-020-0612-3

Liao, J., W. Zheng, Q. Liao, and S. Lu. 2024. Global latitudinal patterns in forest ecosystem nitrous oxide emissions are related to hydroclimate. *npj Climate and Atmospheric Science* 7(1): 187. https://doi.org/10.1038/s41612-024-00737-8

Lloyd, J., and J. A. Taylor. 1994. On the temperature dependence of soil respiration. *Functional Ecology* 8(3): 315–323. https://doi.org/10.2307/2389824

Luo, Y., and X. Zhou. 2006. Preface. In *Soil respiration and the environment*. Academic Press, pp. ix–xi. https://doi.org/10.1016/B978-0-12-088782-8/50000-0

Lützow, M. V., I. Kögel-Knabner, K. Ekschmitt, E. Matzner, G. Guggenberger, B. Marschner, and H. Flessa. 2006. Stabilization of organic matter in temperate soils: Mechanisms and their relevance under different soil conditions – a review. *European Journal of Soil Science* 57(4): 426–445. https://doi.org/10.1111/j.1365-2389.2006.00809.x

Meyer, N., H. Meyer, G. Welp, and W. Amelung. 2018. Soil respiration and its temperature sensitivity (Q_{10}): Rapid acquisition using mid-infrared spectroscopy. *Geoderma* 323: 31–40. https://doi.org/10.1016/j.geoderma.2018.02.031

Okello, J., M. Bauters, H. Verbeeck, S. Bodé, J. Kasenene, A. Françoys, T. Engelhardt, K. Butterbach-Bahl, R. Kiese, and P. Boeckx. 2023. Temperature sensitivity of soil organic carbon respiration along a forested elevation gradient in the Rwenzori Mountains, Uganda. *Biogeosciences* 20(3): 719–735. https://doi.org/10.5194/bg-20-719-2023

Rolka, E., and M. Wyszkowski. 2021. Availability of trace elements in soil with simulated cadmium, lead and zinc pollution. *Minerals* 11(8): 879. https://doi.org/10.3390/min11080879

Schindlbacher, A., C. de Gonzalo, E. Díaz-Pinés, P. Gorría, B. Matthews, R. Inclán, S. Zechmeister-Boltenstern, A. Rubio, and R. Jandl. 2010. Temperature sensitivity of forest soil organic matter decomposition along two elevation gradients. *Journal of Geophysical Research: Biogeosciences* 115: G03018. https://doi.org/10.1029/2009JG001191

Tian, H., R. Xu, J. G. Canadell, R. L. Thompson, W. Winiwarter, P. Suntharalingam, E. A. Davidson, P. Ciais, R. B. Jackson, G. Janssens-Maenhout, M. J. Prather, P. Regnier, N. Pan, S. Pan, G. P. Peters, H. Shi, F. N. Tubiello, S. Zaehle, F. Zhou, and Y. Yao. 2020. A comprehensive quantification of global nitrous oxide sources and sinks. *Nature* 586(7828): 248–256. https://doi.org/10.1038/s41586-020-2780-0

Yi, F., J. Z. Pang, Y. K. Liu, C. H. Peng, S. X. Zhang, L. Hou, X. K. Wang, and H. X. Zhang. 2018. Soil greenhouse gas fluxes (CO_2, CH_4 and N_2O) along a slope of *Pinus tabulaeformis* forest in Qinling Mountains. *Acta Scientiae Circumstantiae* 38(6): 2506–2517.

Zhang, Z.-S., X.-J. Dong, B.-X. Xu, Y.-L. Chen, Y. Zhao, Y.-H. Gao, Y.-G. Hu, and L. Huang. 2015. Soil respiration sensitivities to water and temperature in a revegetated desert. *Journal of Geophysical Research: Biogeosciences* 120(4): 773–787. https://doi.org/10.1002/2014JG002805

Total number of words (including references):5970

Total number of words (excluding references):5262

Abstract number of words:249

Number of words in Supplementary Information:114

Supplementary Files

This is a list of supplementary files associated with this preprint. Click to download.

- ESM1.pdf